Zootaxa 4638 (3): 419–441
https://www.mapress.com/j/zt/

Article

ISSN 1175-5326 (print edition)
ZOOTAXA
ISSN 1175-5334 (online edition)

https://doi.org/10.11646/zootaxa.4638.3.7
http://zoobank.org/urn:lsid:zoobank.org:pub:52D9E9AD-5F2E-4D80-A3B7-5BC3886ABAEA

Delimitation and description of three new species of *Himalopsyche* (Trichoptera: Rhyacophilidae) from the Hengduan Mountains, China

ANNA E. HJALMARSSON
Goethe-University Frankfurt am Main, Institute for Ecology, Evolution and Diversity, Max-von-Laue-Strasse 13, Frankfurt am Main, Germany.
Senckenberg Research Institute and Natural History Museum, Senckenberganlage 25, Frankfurt am Main, Germany.
E-mail: annahjalmar@gmail.com

Abstract

Three new species of the genus *Himalopsyche* (Trichoptera, Rhyacophilidae) from the Hengduan Mountains in China are described. Species delimitation was based on diagnostic features of genitalia, as well as molecular data from six genes analysed using the multi-species coalescent method STACEY. Formal descriptions are focused on genital morphology. Males of *Himalopsyche viteceki* **sp. nov.** are most similar to those of *H. alticola* and *H. martynovi,* and females are most similar to those of *H. tibetana* and *H. velata*. *Himalopsyche immodesta* **sp. nov.** is described based on a single male specimen and it most resembles the males of *H. viteceki*. Males of *H. velata* **sp. nov.** are most similar to *H. tibetana*, and females are most similar to those of *H. maxima* and *H. tibetana*. Diagnostic characters are found on segment IX and the superior and inferior appendages of male genitalia, and most notably on segment VIII in female genitalia. The newly discovered species underline the Hengduan Mountains as a potential source of yet undiscovered aquatic biodiversity.

Key words: caddisfly, freshwater, Himalaya, mountain, Sichuan, STACEY, stream, taxonomy, Yunnan

Introduction

Himalopsyche Banks 1940 is a genus of caddisflies with a Palearctic and circum-Pacific distribution centered around the Hengduan Mountains and the Himalayas and with one species in western North America. The genus *Himalopsyche* was described in the Holarctic family Rhyacophilidae. Relative to most caddisflies, *Himalopsyche* species are large, with the length of each forewing ranging 10–37 mm. The larvae of *Himalopsyche* are free-roaming (i.e., lack the typical caddisfly cases or retreats) and are predators, bearing large mandibles and large and complex abdominal gills (Flint 1961; Graf & Sharma 1998; Lepneva 1970; Saito 1965; Tanida 1985; Thamsenanupap *et al*. 2005).

Phylogenetic hypotheses have been formulated for *Himalopsyche* by Ross (1956), Schmid & Botosaneanu (1966), Saini & Kaur (2011), and Hjalmarsson *et al*. (2019). Recently, Hjalmarsson *et al.* (2019) evaluated and revised the phylogenetic hypotheses and species groups formulated by previous workers, defining five species groups in *Himalopsyche*: *H. kuldschensis* Group, *H. navasi* Group, *H. tibetana* Group, and the monotypic *H. lepcha* and *H. phryganea* Groups.

There is generally much morphological variation in male genital structures within *Himalopsyche*, but some *Himalopsyche* species are quite similar to one another, representing potential species complexes. For example, Ross (1956) referred to the following complexes: *H. alticola-martynovi*-Complex, *H. placida-excisa*-Complex, and *H. tibetana-biansata-fasciolata*-Complex. Since then, more species have been described, and judging from their morphology, *H. epikur* Malicky 2011 can be assigned to the *H. martynovi*-Complex together with *H. martynovi* Banks 1940 and *H. alticola* Banks 1940, and *H. maitreya* Schmid 1963 can be assigned to the *H. excisa*-Complex together with *H. excisa* Ulmer 1905 and *H. placida* Banks 1947. The *H. martynovi*-Complex occurs in the Hengduan Mountains and the currently recognized species show high morphological variation, making it difficult to differentiate between inter- and intraspecific morphological variability. I encountered specimens of *Himalopsyche*

Accepted by J. Morse: 17 May 2019; published: 17 Jul. 2019

from the Hengduan Mountains in China that were relatively similar to the species of the *H. martynovi*-Complex and *H. tibetana* (Martynov 1930), respectively. But their genital male morphology was distinct, so I hypothesized that they represent yet-undescribed species for science.

Of the hitherto described 53 *Himalopsyche* species, 29 have been described as females (Banks 1940; Forsslund 1935; Hsu 1997; Kawai & Tanida 2005; Kimmins 1952; Lakhwinder & Saini Malkiat 2015; Malicky 1978; Schmid 1969; Schmid & Botosanean 1966), with the major contributions done by Kimmins (1952) and Schmid & Botosaneanu (1966); of these, 3 have been described exclusively as females (*H. elegantissima* (Forsslund 1935), *H. maxima* (Forsslund 1935) and *H. schmidi* Lakhwinder & Saini 2015). Although less conspicuous than male genital morphology, the genital morphology of *Himalopsyche* females is variable and distinct, making species determination based on female specimens possible.

Molecular analysis is a powerful tool to aid and standardize integrative taxonomy (Schlick-Steiner *et al*. 2010; Vitecek *et al*. 2017). Multispecies coalescent methods offer the most realistic species tree models to date (Rannala 2015), and enable multilocus species delimitation without assuming monophyly of gene trees (e.g., Fujisawa & Barraclough 2013; Zhang *et al*. 2013). Instead, a joint probability for the gene trees, species tree, and species delimitation is calculated. In this study I wanted to assess if multi-locus coalescent approaches can help resolve the status of recognized and putative species in *Himalopsyche*. I used molecular species delimitation with STACEY to test if the seemingly different populations represent independently evolving lineages, and posit that these morphologically distinct populations represent independent evolutionary lineages that are hitherto unrecognized species. Three new species were recognized based on their unique morphological and molecular properties and are here described.

Materials and methods

Specimens of the new species were collected with light traps during a field campaign in the Hengduan Mountains, China. Comparative material was either collected in the field or borrowed from the private research collection of Hans Malicky in Lunz am See, Austria, or from the Museum für Naturkunde in Berlin, Germany (Table S1). Specimens were either kept in 95% alcohol or dry on pins. Male genitalia were examined after clearing in lactic acid (Blahnik *et al*. 2007). For examination and illustration of each specimen, cleared genitalia were kept in glycerin and placed on a small piece of cotton wool soaked in glycerin (very carefully because cotton wool can easily destroy the specimen if not handled with care) on a cavity microscope slide together with tiny glass balls soaked in glycerin to keep the genitalia stable. Genitalia were examined using an Olympus SZX7 stereoscope and were illustrated as follows. Structures were traced in pencil using a Leitz Dialux 20 microscope at 100x magnification with a mounted drawing tube. Pencil sketches were then scanned and used as templates for digital 'inking' in Adobe Illustrator. Reproductory tract organs such as aedeagus, paramere, and bursa copulatrix (vaginal apparatus) were not removed from the animals, and were generally drawn while inside the abdomen. This limited the level of detail provided of the illustrations of these body parts, but conserved physical integrity of holotypes and paratypes. As an exception, the bursa copulatrix of the *H. velata* **sp. n.** female was drawn outside of the abdomen, since the reproductive organ loosened and fell out of the abdomen after clearing.

The following seven gene fragments were PCR-amplified and sequenced: 16S mitochondrial rRNA, 28S nuclear rRNA, CAD nucDNA, Cytochrome C Oxidase subunit I (COI) COI-5P and COI-3P mtDNA, RNA Polymerase II (RPB2) nucDNA, and Wingless (Wnt1) nucDNA. The COI fragment COI-5P is the 'standard barcode' fragment, close to the 5' end of the gene, and upstream of the COI-3P fragment (Table 1). DNA was extracted from legs using either Qiagen Dneasy Blood & Tissue Kit or Qiagen QIAamp DNA Micro Kit. A large proportion of material came from museum collections and had been stored up to 23 years before DNA extraction. The oldest samples from which I successfully amplified DNA were pinned dry specimens collected in 1993. The bulk of the material used had been stored in 70%–95% ethanol, and the oldest specimen in ethanol from which I amplified DNA had been collected in 1994. All material borrowed from Museum für Naturkunde in Berlin was pinned dry, all material borrowed from Hans Malicky was stored in 70% ethanol at room temperature, and all material stored in Senckenberg Research Institute (Frankfurt am Main and Müncheberg) is kept in 95% ethanol and is kept frozen. DNA tends to fragment over time, so I developed primers for short amplicons to allow amplification of fragmented DNA (Table 2), and worked with small elution volumes (e.g., 35 µL) to obtain high DNA concentrations. For 10µL Polymerase Chain Reactions (PCR), I used VWR peqGOLD 'Hot Start' Taq-DNA-Polymerase, VWR buffer Y or S VWR, and, for

some reactions, added Bovine serum albumin (BSA) or Dimethyl sulfoxide (DMSO). Sets of deoxyribonucleotide triphosphates (dNTPs) were used from the ThermoFischer dNTP set. Detailed PCR protocols are published elsewhere (Hjalmarsson *et al*. 2019). DNA sequences were aligned with the Mafft algorithm implemented in AliView (Katoh *et al*. 2002; Larsson 2014). The molecular dataset included 119 individuals of species from the *H. tibetana* Group (*sensu* Hjalmarsson *et al.* 2019), as well *H. lepcha* Schmid 1963 (Table S1) The total alignment length was 4370 bp (Table 1). All molecular data are uploaded to the BOLD database (www.boldsystems.org) in the project SPHIM; all samples included in the study are marked with 'Hdescr' in the 'Extra Info' field in BOLD (Table S1).

TABLE 1. Molecular data for STACEY species delimitation.

Gene fragment	Number of Sequences	Alignment Length	Variable Characters	Parsimony Informative Characters	Missing Data/Gaps
16S	100	336	20%	19%	3.3%
28S	84	972	3.5%	3.2%	7.3%
CAD	89	850	19%	17%	5.9%
COI-5P	110	502	31%	38%	3.5%
COI-3P	106	541	35%	32%	3.5%
RPB2	99	802	15%	13%	7.2%
Wnt1	85	367	28%	23%	0.6%

Molecular species delimitation was performed using STACEY (Jones *et al*. 2015; Jones 2017), which is a modification of *BEAST and runs as an add-on to BEAST (Bouckaert *et al*. 2014). Species delimitation with STACEY follows a two-step procedure. First, species tree estimation is performed in STACEY. Second, species delimitation is performed using SpeciesDelimitationAnalyser (Jones *et al*. 2015; Jones 2017). Just like *BEAST, STACEY is based on the multispecies coalescent model (Yang & Rannala 2010). In addition, it uses a 'birth-death-collapse' model that includes a collapse parameter that has a distribution with a peak near zero so that some branches can be virtually collapsed, indicating that the leaves attached to the branches are conspecific (Jones *et al*. 2015). This makes it possible to include all species delimitation scenarios in a single Bayesian parameter space, without having to use reversible-jump MCMC to sample from separate parameter spaces with different dimensionalities.

For STACEY, alignments were partitioned by gene and codon position, and substitution rates were unlinked among these partitions. I defined five separate gene trees: one for each nuclear gene, and one for all mitochondrial gene fragments. Model selection was done with bModeltest (Bouckaert & Drummond 2017) which estimates the substitution models simultaneously with the Bayesian tree search. I used the transition/transversion split option, and used empirical base frequencies. All trees were estimated under a Lognormal Relaxed Clock.

The 'birth-death-collapse' tree model of STACEY has the following parameters: collapse height ε, speciation rate λ, extinction rate μ, collapse weight ω, and origin height t. Prior distributions of parameters were set in BEAUTi (Bouckaert *et al*. 2014) as follows: Speciation rate (bdcGrowthRate), log normal distribution, M = 3, S = 1.5, min = 1.0E-99, max = 1.0E99, initial = 0.02; population size (popPriorScale), log normal distribution, M = 3, S = 1.5, min = 1.0E-99, max = 1.0E99, initial = 0.02. All other priors were left at default values. The ploidy was set to 2 for all loci (Jokusch *et al*. 2014). SpeciesDelimitationAnalyser (Jones *et al*. 2015) was executed with a collapse height set to 0.01 (1/10 of average branch length of the output tree, Jones *et al*. 2015). Two independent Bayesian 'burn-in' Markov chain Monte Carlo (MCMC) runs were generated for 0.5 billion generations. From the end point of these two runs, two new runs each were started, sampling for 0.5 billion generations. The runs were concatenated so that two independent tree samples were generated with a total of 1 billion of MCMC generations each.

Results

Species delimitation results from two independent tree samples were identical, yielding 17 delimited taxa (Table 3, Figures 1, S1). The fractions of the most common species delimitations were 11% and 7%, respectively. The putatively new species were confirmed to represent independently evolving lineages and are described below. The STACEY analysis was congruent with established taxonomy for the remaining species, with the exception of the

H. excisa-Complex (*H. excisa*, *H. maitreya*, and *H. placida*), and the *H. martynovi*-Complex which were unresolvable with the data at hand. *Himalopsyche martynovi* is morphologically similar to *H. alticola* and *H. epikur*. In the STACEY analysis, these three species were represented in two clades which were delimited to each represent an independently evolving lineage, but both had a posterior probability below 90% so they cannot be regarded as each being monophyletic with certainty. One of these clades had a posterior probability of 84% and only included specimens determined as *H. epikur*, so I designate this clade to *H. epikur*. The other clade had a posterior probability of 82% and entailed specimens determined as *H. martynovi*, *H. alticola*, and *H. epikur*, and I designate this clade as the *H. martynovi*-Complex containing the species *H. martynovi*, *H. alticola*, and *H. epikur.* The morphological variability within the *H. martynovi*-Complex was large and is discussed below (Figure 7). The analysis also delimited three taxa of unknown species identity as separate taxa, *H.* sp. 0044 (F, L) *H.* sp. 1338 (L), and *H.* sp. 1254 (L). For these species only larvae and females were available in our sampling (Hjalmarsson *et al*. 2018).

TABLE 2. Primers used in the study.

Gene	Name	Length	Direction	Sequence 5' to 3'	Reference
16S	L1F	23	forward	AGACTGGAATGAATGATT-GGACG	Hjalmarsson *et al*. 2019
16S	L2Fa	20	forward	TGGTTGGGGTGATCTTGAAA	Hjalmarsson *et al*. 2019
16S	L2Ra	20	reverse	TTTCAAGATCACCCCAACCA	Hjalmarsson *et al*. 2019
16S	L3R	23	reverse	ACGCTGTTATCCCTAAGGTATCT	Hjalmarsson *et al*. 2019
16S	LeptoF	18	forward	TAAGTGTGCAAAGGTAGC	Johanson & Malm 2010
16S	LeptoR	19	reverse	TTAATCCAACATCGAGGTC	Johanson & Malm 2010
28S	D1-3up1_a	24	forward	CGAGTAGCGGCGAGCGAAACG-GGA	This work (Modified from Vitecek *et al*. 2015: 5'-CGAGTAGCG-GCGAGCGAACGGA)
28S	D2dnB	21	reverse	CCTTGGTCCGTGTTTCAAGAC	Zhou *et al*. 2007
28S	D2up4	23	forward	GAGTTCAAGAGTACGTGAAAC-CG	Zhou *et al*. 2007
28S	D3-TRIC-DN	21	reverse	ATTCCCCTGACTTCGACCTGA	Vitecek *et al*. 2015
CADH	1028r-ino	23	reverse	TTRTTIGGIARYTGICCICCCAT	Johanson & Malm 2010
CADH	743nF-ino	26	forward	GGIGTIACIACIGCITGYTTYG-ARCC	Johanson & Malm 2010
CADH	C1-Fb	20	forward	TGYGTTGTRAAGATTCCGAG	Hjalmarsson *et al*. 2018
CADH	C2-Ra	20	reverse	TTATCAGTGGGCTCTTGCAG	Hjalmarsson *et al*. 2019
CADH	C3-Fb	19	forward	TGATTTTCATGTCGTATTGG	Hjalmarsson *et al*. 2019
CADH	C6-Fa	20	forward	AATGGCCKGCGAGTACAAAC	Hjalmarsson *et al*. 2019
CADH	C6-Ra	20	reverse	TAGAGATAGTTTGTACTCGC	Hjalmarsson *et al*. 2019
CADH	C7-Ra	20	reverse	TGTCCATTACAACCTCGAATG	Hjalmarsson *et al*. 2018
COI-3P	J1F	22	forward	TTYTHATTYTMCCWGGATTYGG	Hjalmarsson *et al*. 2019
COI-3P	J3F	20	forward	ATTTTYAGRTGATTAGCHAC	Hjalmarsson *et al*. 2019
COI-3P	J3R	20	reverse	GTDGCTAATCAYCTRAAAAT	Hjalmarsson *et al*. 2019
COI-3P	J6R	20	reverse	AAAGGGTTTAGAGTAAGACC	Hjalmarsson *et al*. 2019
COI-3P	Jerry	23	forward	CAACATTTATTTTGATTTTTTGG	Simon *et al*. 1994
COI-3P	S20	23	reverse	GGGAAAAAGGTTAAATT-TACTCC	Pauls *et al*. 2003, 2006
COI-5P	B1-Fa	20	forward	ATTGCDACWGATCAWACAAA	Hjalmarsson *et al*. 2018
COI-5P	B2-Fa	20	reverse	CCWGTWCCYGCTCCRTTTTC	Hjalmarsson *et al*. 2019
COI-5P	B2-Ra	20	forward	GAAAAYGGAGCRGGWACWGG	Hjalmarsson *et al*. 2019
COI-5P	B3-Ra	20	reverse	AAYGTARTWGTWACWGCTCA	Hjalmarsson *et al*. 2018
COI-5P	B4-Rc	20	reverse	TTTATYTTAGGDATYTGAGC	Hjalmarsson *et al*. 2019

.....continued on the next page

TABLE 2. (Continued)

Gene	Name	Length	Direction	Sequence 5' to 3'	Reference
COI-5P	HCO2198	26	reverse	TAAACTTCAGGGTGAC-CAAAAAATCA	Folmer *et al*. 1994
COI-5P	LCO1490	25	forward	GGTCAACAAATCATAAAGA-TATTGG	Folmer *et al*. 1994
COI-5P	LEP-F1	22	forward	ATTCAACCAATCATAAAGATAT	Hebert *et al*. 2004
COI-5P	LEP-R1	22	reverse	TAAACTTCTGGATGTCCAAAAA	Hebert *et al*. 2004
RPB2	P1-F	20	forward	AAGCCCAAACCTTTGTGGAC	Hjalmarsson *et al*. 2019
RPB2	P3-F	20	forward	CGGCGAGCTTATCATGGGTA	Hjalmarsson *et al*. 2019
RPB2	P3-R	20	reverse	TACCCATGATAAGCTCGCCG	Hjalmarsson *et al*. 2019
RPB2	P5F	20	forward	GCTGATCCCCAGACTTACCG	Hjalmarsson *et al*. 2019
RPB2	P6-R	20	reverse	ATTACCTGGGGTGGGTTCCA	Hjalmarsson *et al*. 2019
RPB2	P7-F	20	forward	ATTGCCTGTGTGGGTCAACA	Hjalmarsson *et al*. 2019
RPB2	P7-R	20	reverse	TGTTGACCCACACAGGCAAT	Hjalmarsson *et al*. 2019
RPB2	POLFOR2	23	forward	TGGGAYGSYAAAATGCCK-CAACC	Danforth *et al*. 2006
RPB2	POLREV2	26	reverse	TYYACAGCAGTATCRATRAGAC-CTTC	Danforth *et al*. 2006
Wnt1	W1-Fb	20	forward	ATCATTYCGCACTATWGGAG	Hjalmarsson *et al*. 2019
Wnt1	W4-Fa	19	forward	AARCCRCACAAYCCRGARC	Hjalmarsson *et al*. 2019
Wnt1	W4-Ra	20	reverse	TCYGGRTTGTGYGGYTTYAG	Hjalmarsson *et al*. 2019
Wnt1	W6-Ra	19	reverse	GCATCTCTCGACGACGGTC	Hjalmarsson *et al*. 2019

TABLE 3. Summary of STACEY results

STACEY cluster	Included morphospecies	Samples
H. anomala	*H. anomala*	3 males, 1 larva
H. auricularis	*H. auricularis*	2 males
H. digitata	*H. digitata*	3 males, 4 larvae
H. eos	*H. eos*	2 males
H. epikur	*H. epikur*	5 males, 8 females
H. excisa-Complex	*H. excisa*, *H. maitreya, H. placida*	17 males
H. gregoryi	*H. gregoryi*	5 males, 3 females
H. immodesta	*H. immodesta*	1 male
H. lepcha	*H. lepcha*	5 males
H. martynovi-Complex	*H. martynovi* (and potentially also *H. alticola* and *H. epikur*)	9 males, 1 female
H. platon	*H. platon*	1 male
H. tibetana	*H. tibetana*	4 males, 4 females, 14 pupae
H. velata	*H. velata*	4 males, 1 female
H. viteceki	*H. viteceki*	5 males, 3 females
H. sp 44 (F, L)	-	2 larvae, 9 females
H. sp. 1196 (L)	-	3 larvae
H. sp. 1254 (L)	-	1 larva

Taxonomy

The terminology I use is an English version of the one used by Schmid & Botosaneanu (1966) and Schmid 1970, except for the dorsomesal process in males of *H. velata*, which I here define as a posterior dorsomesal process extending from segment IX. Also I refer to the "App. Preanaux" *sensu* Schmid & Botosaneanu (1966) as the superior appendages.

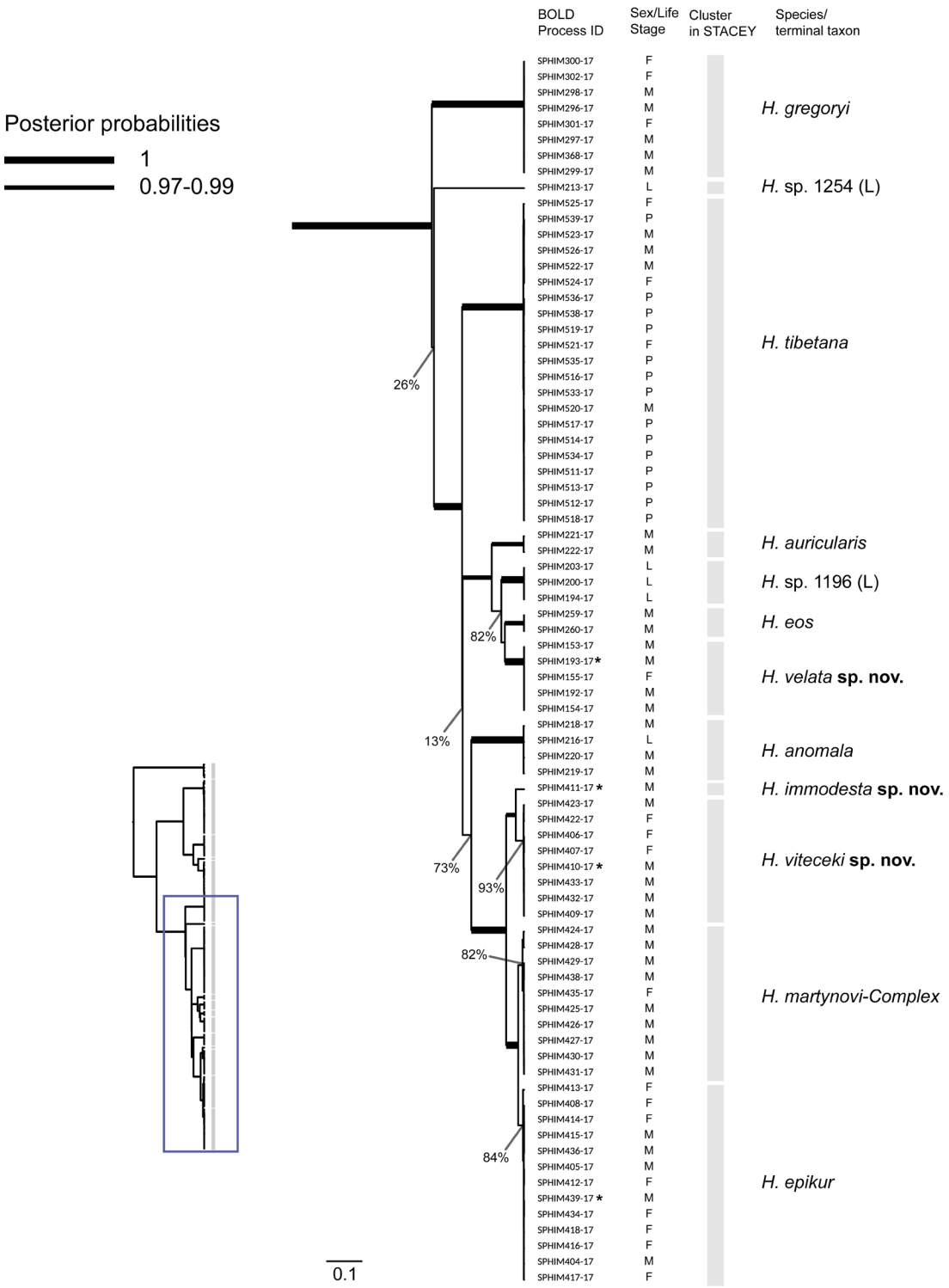

FIGURE 1. Species tree and species delimitation hypothesis generated with STACEY and SpeciesDelimitationAnalyser; delimited clusters are indicated by grey boxes. Thick branches indicate clades with a posterior probability of at least 97%; nodes with lower posterior probabilities are annotated. Posterior probabilities for nodes within clusters delimited with STACEY are not shown. The Figure shows a part of the complete topology, as indicated by the miniature tree; the complete topology can be found in Figure S1. Sexes/Life stages are denoted as follows. F = female; L = larva; M = male; P = pupa. Scale bar indicates number of substitutions per unit branch length. Asterisks denote holotypes.

Terminology and abbreviations
Males
IX = Abdominal segment IX
X = Tergum X
dm.p. = Dorsomesal process
s.a. = Superior appendages
a.s. = Anal sclerites
i.e. = Inferior appendages
a = Aedeagus
p = Paramere
Females
VIII = Abdominal segment VIII
IX = Tergum IX
X = Tergum X
vm.p. = Ventromesal process of segment VIII
b.c. = Bursa copulatrix

***Himalopsyche viteceki* sp. nov.**
Figures 2A–2E, 3A–3C

Material examined. Holotype. 1 male: China, Yunnan, Diqing Tibetan Autonomous Prefecture, Dêqên County, Yakou, Baima Snow Mountain, 28°18.09'N, 99°8.60'E, ca 3430 m asl; leg. Chen, Hjalmarsson, Li, 30.vii.2013. Deposited in Senckenberg Research Institute, Frankfurt am Main, Germany. BOLD Process ID SPHIM410-17, Field ID AH0683, Museum ID SMFTRI00017216.

Paratypes. 4 males, 2 females: Same collection data as holotype. Deposited in Senckenberg Research Institute, Frankfurt am Main, Germany (SMFTRI00017215, SMFTRI00018190, SMFTRI00018191, SMFTRI00017212, SMFTRI00017213) and Senckenberg Deutsches Entomologisches Institut, Müncheberg, Germany (SMFTRI00018192). 1 female: Myanmar, Kachin Hills, leg. S. Naumann, 3.x.2010. Stored in Museum für Naturkunde, Berlin, Germany.

Diagnosis. Males of the new species are most similar to those of *H. alticola, H. martynovi*, and *H. immodesta* **sp. nov.**, but (1) superior appendages each without a distinct incision between mesal and lateral lobes (with a distinct incision in *H. alticola*, *H. martynovi*, and *H. immodesta* **sp. nov.**); (2) the ventrocaudal margin of the lateral lobe of each superior appendage is straight with a mesal triangular protrusion (concave in *H. alticola*, pointed in *H. martynovi*); (3) the mesodorsal margin of each superior appendage has an oval tip lacking a ventral triangular protrusion (oval tip with ventral triangular protrusion in *H. immodesta* **sp. nov.**); (4) the tip of the distal segment of each inferior appendage is subrhombic and projecting mesodorsad in an obtuse angle (the tip of the distal segment is suboval in *H. martynovi* and subrhombic, but projecting perpendicularly mesodorsad in *H. immodesta* **sp. nov.**). Females of the new species are most similar to *H. tibetana* and *H. velata* **sp. nov.**, but (1) in lateral view, segments IX and X seemingly are fused, with IX forming lateral tongue-like sclerites projecting ventrad (IX triangular in *H. tibetana*, IX completely fused with X in *H. velata* **sp. nov.**); (2) in ventral view, the center of the ventral margin is elevated and forming a narrow, finger-like ventromesal process (elevated and forming a triangular protrusion in *H. tibetana* and *H. velata*); (3) the posterior margin of VIII has a posterior lobe in the ventral portion (posterior margin of VIII without such lobe in *H. tibetana* and *H. velata*); (4) segment VIII in lateral view has a ventromesal protuberance in the caudal portion (without a ventromesal protuberance in *H. tibetana* and *H. velata*); (5) the ventromesal lobes are short, stout, and projecting dorsad (ventromesal lobes elongate and finger-like in *H. velata*).

Description. *Adults*. Habitus (in alcohol) dark; sternites beige, tergites dark; legs beige with dark stripes. Wings with dark pattern and dark setae on veins. Male maxillary palps each 5-segmented, spur formula 3-4-4. Length of each forewing in males 18–20 mm, in females 22–24 mm.

Male genitalia (Figure 2). Segment IX dorsally longer than ventrally and seemingly fused with tergum X; in dorsal view anteriorly concave, lateral margins slightly convex, caudally with pair of shallow mesolateral incisions at base of processes of tergum X (Figure 2D); segment IX in lateral view dorsally slightly convex, caudal margin

dorsal portion straight with distinct small dorsal indentation at base of tergum X and ventral portion deeply incised (2/3 of segment length) at insertions of inferior appendages (Figure 2A); in ventral view anteriorly straight with two shallow sublateral indentations, caudally obtusely convex (Figure 2E). Tergum X with deep mesal incision forming two parallel ridges; in dorsal view elongate subtriangular with deep mesal incision (Figure 2D); in lateral view projecting dorsad in oblique angle from segment IX, dorsal margin convex and connected with anal sclerites and superior appendages by membranous structure (Figure 2A). Anal sclerites not fused (Figure 2D); in lateral view sinuous, hooked ventrad apically (Figure 2A). Superior appendages complex, each laterally compressed and in lateral view planar, indistinctly bilobed, approximately as long as inferior appendages (Figure 2A); their mesodorsal lobes in lateral view each evenly curved with oval tip and projecting caudoventrad, in dorsal view digitate (Figures 2A, 2D); each lateral lobe laterally compressed and planar, its dorsal margin fused with mesodorsal lobe, in lateral view with dorsocaudal margin concave, ventrocaudal margin straight with mesal triangular protrusion, ventral margin straight with very indistinct concavity (Figure 2A), in dorsal and ventral views with triangular subterminal protrusion projecting mesad (Figures 2D, 2E). Inferior appendages each 2-segmented: Basal segment bilobed, mesodorsal lobe in lateral view acute-oval with subterminal ventral indentation, lateroventral lobe digitiform; distal segment dorsally longer than ventrally, tip of distal segment in lateral view subrhombic, projecting mesodorsad with fine dense thorns on mesal face (Figure 2A). Aedeagus positioned dorsally and on left side of paramere, sinuous, wider at base, tapering towards apex, apex projecting ventromesad; in lateral view sinuous, apex projecting ventrad with small opening on ventral face of apex; in ventral view wide with distinct angle at 2/3 of its length, caudal third pipe-shaped, curving mesad, with opening semi-circular (Figures 2B, 2C). Paramere spinose, somewhat shorter than aedeagus, in ventral view with rounded base (Figures 2B, 2C).

Female genitalia (Figure 3). Segment VIII synsclerous, not divided into tergite and sternite, in dorsal view anteriorly broader than caudally, anterior margin straight, lateral corners with protrusions, lateral margins straight, oblique, caudal margin broadly incised and with rounded lateral corners (Figure 3B); in lateral view dorsal margin straight, caudal margin with dorsal portion rounded, mesal portion straight, and ventral portion forming lobes projecting caudad and connected to pair of strong ventromesal lobes projecting caudad and covered with fine pubescent hair, ventromesal process ventral to the ventromesal lobes and projecting dorsocaudad from segment VIII, about half as long as ventromesal lobes and with long, thick setae, ventral margin of VIII in lateral view straight, oblique, with mesal protuberance in caudal portion (Figure 3A); segment VIII in ventral view anterior margin slightly convex with two pairs of sublateral anterior protrusions, lateral margins straight and sweeping inward caudally, caudal margin with deep incisions between ventrolateral lobes and ventromesal lobes, ventrolateral lobes in ventral view narrow and projecting mesocaudad, ventromesal lobes digitiform and projecting laterocaudad, ventromesal process digitiform and 1/3 as long as ventromesal lobes (Figure 3C). Ventromesal lobes thick and covered with very short, pubescent hair, in lateral view dorsal margins convex, ventral margins concave, in ventral view finger-like and projecting caudolaterad (Figure 3A). Segment IX indistinct, lightly sclerotized and dorsally fused with segment X, in lateral view tongue-shaped and projecting slightly ventrad (Figures 3A, 3B). Segment X membranous with distinct pair of sclerotized patches dorsmesally, and pair of smaller sclerotized patches basolateral of the larger pair (Figures 3A, 3B); dorsal lobes each with small pair of cerci projecting caudad (Figures 3A–C). Apodemes extending from segment X through segment VIII, extending anterad (Figures 3A, 3B). Bursa copulatrix as pictured with dotted outline in dorsal and lateral views (Figures 3A, 3B).

Etymology. Named for Simon Vitecek, entomologist.

Distribution. China (Yunnan); Myanmar (Figure 8A).

Himalopsyche immodesta sp. nov.

Figures 4A–4E

Material examined. Holotype. 1 male: China, Yunnan, Dali Bai Autonomous Prefecture, small stream 5 km NW of Fengyu town, 26°1.31'N, 99°53.28'E, ca 2730 m asl; leg. Chen, Hjalmarsson, Li, 23.vii.2013. Deposited in Senckenberg Research Institute, Frankfurt am Main, Germany. BOLD Process ID SPHIM411-17, Field ID AH0685, Museum ID SMFTRI00017218.

Additional material. 33 larvae: Yunnan, China: 27°37.95'N, 99°22.09'E (28 larvae); 26°19.38'N, 99°15'E (3 larvae); 26°19.49'N, 99°16.67'E (2 larvae). Deposited in Senckenberg Research Institute, Frankfurt am Main, Germany (Table S1).

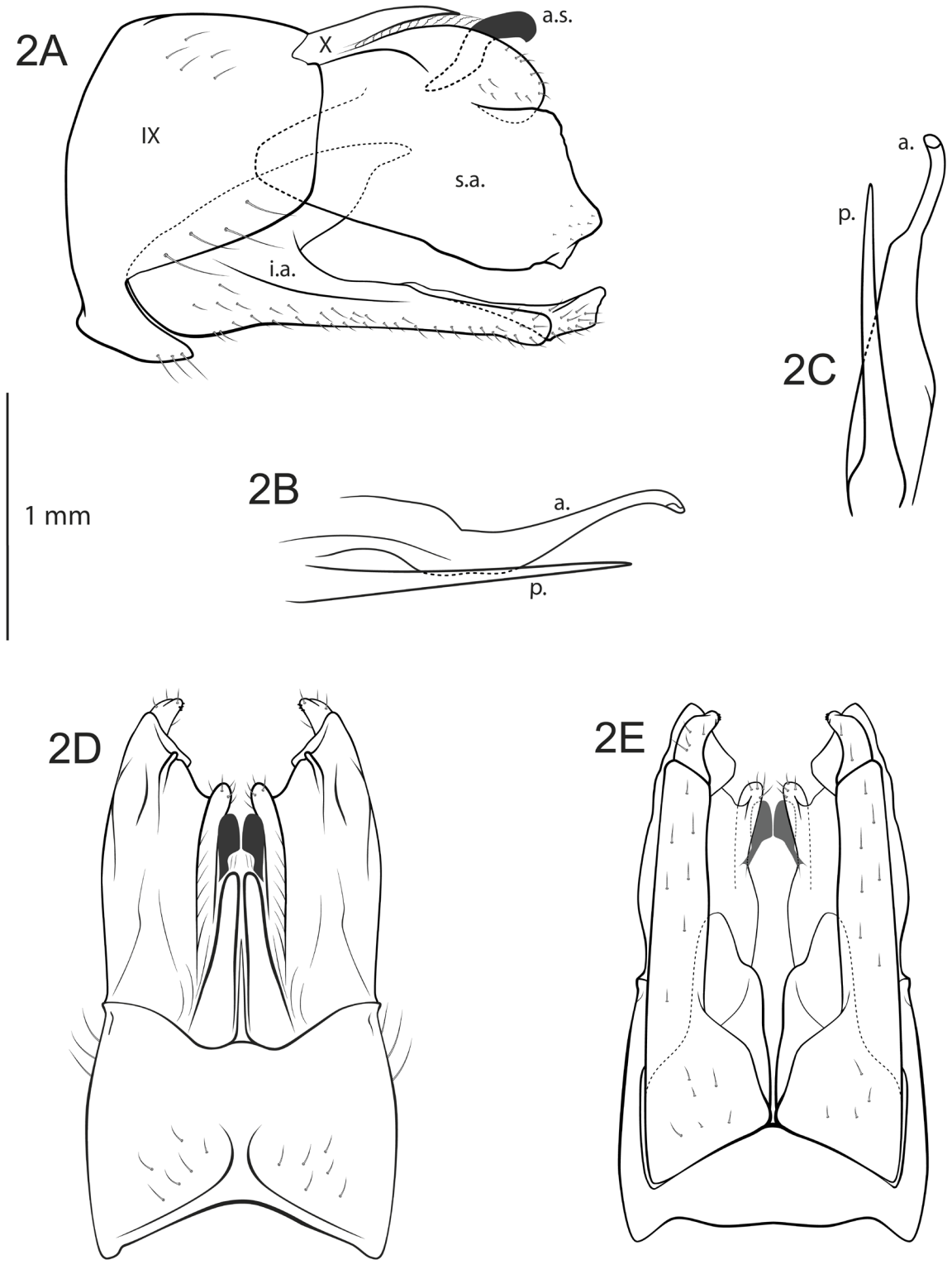

FIGURE 2. Male genitalia of *Himalopsyche viteceki* **sp. n.** 2A, left lateral; 2B, phallic apparatus, left lateral; 2C, phallic apparatus, ventral; 2D, dorsal; 2E, ventral. Abbreviations: IX = abdominal segment IX; X = tergum X; a.s. = anal sclerite; s.a. = superior appendages; i.a. = inferior appendages; a. = aedeagus; p. = paramere.

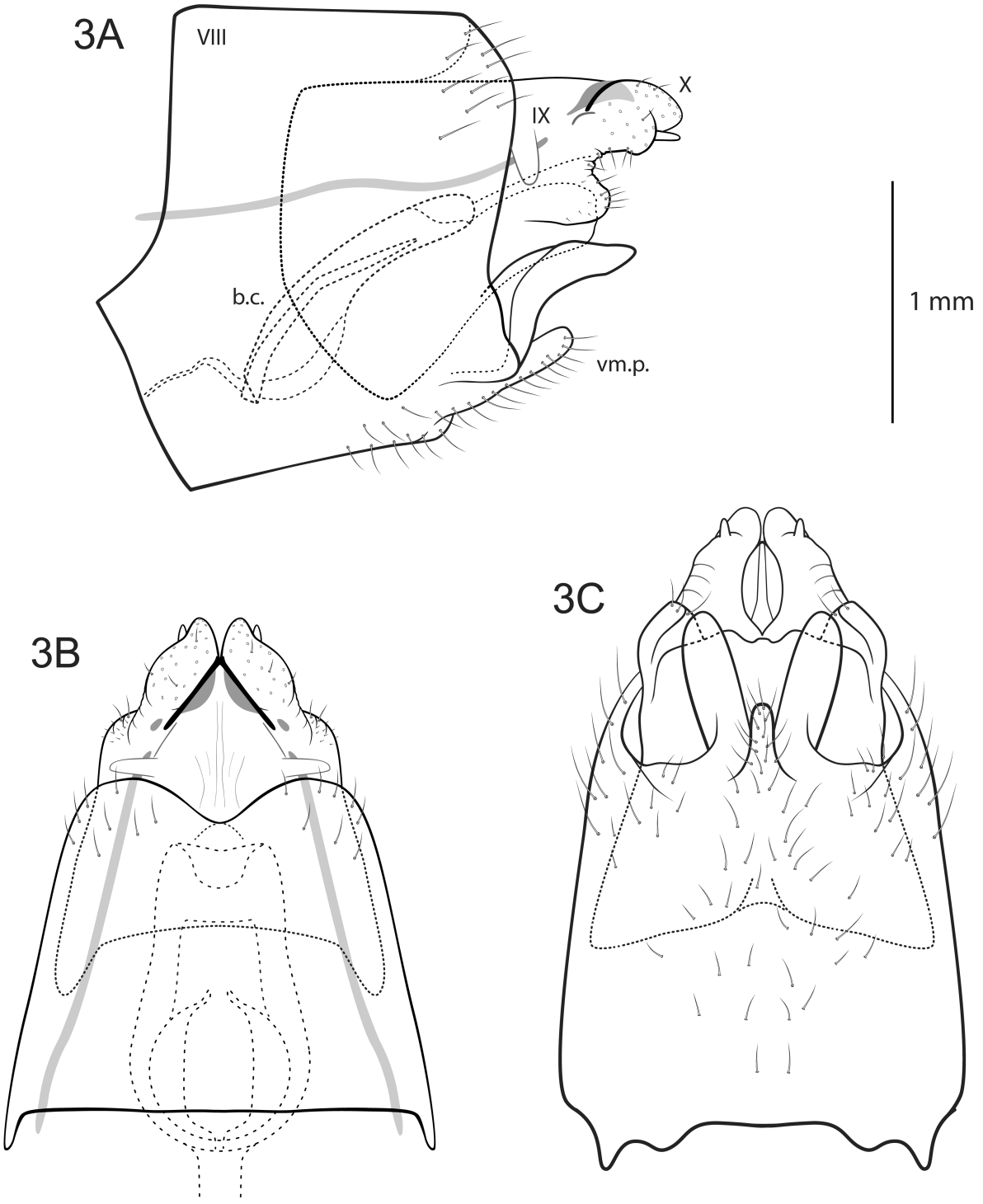

FIGURE 3. Female genitalia of *Himalopsyche viteceki* **sp. n.** 3A, left lateral; 3B, dorsal; 3C, ventral. Abbreviations: VIII = abdominal segment VIII; IX = tergum IX; X = tergum X; b.c. = bursa copulatrix; vm.p. = ventromesal process of segment VIII.

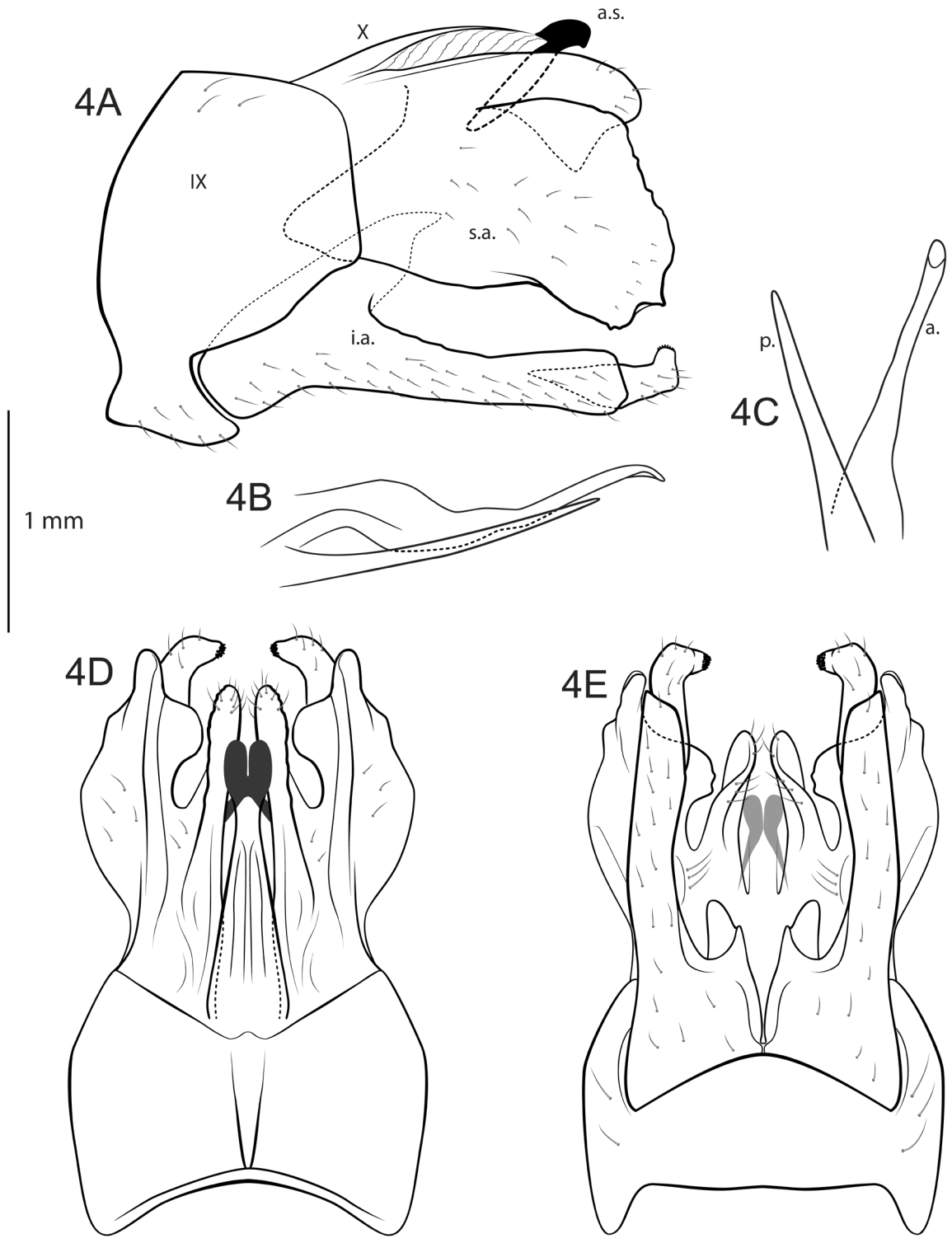

FIGURE 4. Male genitalia of *Himalopsyche immodesta* **sp. n.** 4A, left lateral; 4B, phallic apparatus, left lateral; 4C, phallic apparatus, ventral; 4D, dorsal; 4E, ventral. Abbreviations: IX = abdominal segment IX; X = tergum X; a.s. = anal sclerite; s.a. = superior appendages; i.a. = inferior appendages; a. = aedeagus; p. = paramere.

Diagnosis. The holotype of the new species is most similar to the male of *H. viteceki*, but (1) the mesodorsal lobe of each superior appendage has a ventral triangular protrusion in lateral view (absent in *H. viteceki*); (2) the distal segment of each inferior appendage is 1/3 as long as the proximal segment and the tip of the distal segment is

curved mesad at a right angle, projecting distinctly mesodorsad (the distal segment is half as long as the proximal segment and the tip of the distal segment is subrhombic, projecting mesodorsad in an oblique angle in *H. viteceki*); (3) lateral lobes of superior appendages laterally convex in dorsal/ventral views and with clear caudal incision between the mesodorsal and lateral lobes in dorsal/ventral views (the lateral lobes of the superior appendages are straight, bending slightly inward in dorsal/ventral views and without caudal incisions between the mesodorsal and lateral lobes in dorsal/ventral views in *H. viteceki*).

Description. *Adults*. Habitus (in alcohol) brown; sternites beige, tergites brown; legs beige with dark stripes. Wings with brown pattern and dark setae on veins. Male maxillary palps each 5-segmented, spur formula 3-4-4. Length of each forewing in males 19–21 mm.

Male genitalia (Figures 4A–4E). Segment IX dorsally longer than ventrally and seemingly fused with tergum X; in dorsal view anteriorly concave, lateral margins convex, caudally concave with small dorsomesal process projecting caudad (Figure 4D); in lateral view dorsal margin slightly convex, caudal margin with dorsal portion straight, slightly oblique, ventral portion irregularly deeply incised (2/3 of segment length) at insertions of inferior appendages (Figure 4A); in ventral view anteriorly straight, caudally convex (Figure 4E). Tergite X forming two parallel ridges projecting in oblique angle dorsad from segment IX, tapering towards apices and fused with anal sclerites apically, in dorsal view elongate subtriangular; in lateral view dorsal margin convex and ventral margin joined with a membranous structure (Figures 4A, 4D). Anal sclerites fused mesally (Figure 4D); in lateral view with basal portion straight, tip hooked ventrad (Figure 4A). Superior appendages each complex, planar, indistinctly bilobed and approximately as long as inferior appendages; mesodorsal lobe in lateral view evenly curved and projecting caudoventrad with oval tip and large ventral triangular protrusion (Figure 4A), in dorsal view digitiform and fused with lateral lobe (Figure 4D); lateral lobe foliaceous, large, in lateral view dorsal margin fused with mesodorsal lobe, dorsocaudal margin unevenly convex, ventrocaudal margin concave, ventral margin with protrusion in caudal half (Figure 4A), in dorsal and ventral views lateral margins convex, with clear caudal incision between mesodorsal and lateral lobes and with irregularly rounded mesal intrusion (Figures 4D, 4E). Inferior appendages each 2-segmented: Basal segment bilobed, mesodorsal lobe acute with subterminal caudoventral indentation; lateroventral lobe digitiform, distally slightly dilating; distal segment 1/3 as long as proximal segment and with subrectangular tip projecting distinctly mesodorsad in right angle, with fine dense thorns on mesal face (Figures 4A, 4E) . Aedeagus positioned on left side of paramere; in lateral view irregularly sinuate, wider at base; in ventral view projecting laterocaudad, with oval opening (Figures 4B, 4C). Paramere spiniform, shorter and thinner than aedeagus, in ventral view projecting laterocaudad (Figures 4B, 4C).

Etymology. The name refers to the ornate and ostentaceous (immodest) shape of the male genitalia.

Distribution. China (Yunnan; Figure 8A).

*Himalopsyche velata s*p. nov.

Figures 5A–5E, 6A–6E

Material examined. Holotype. 1 male: China, Sichuan, Garzê Tibetan Autonomous Prefecture, small stream 4 km E of Dongmoyong village, 29°6.96'N, 100°1.96'E, ca. 4150 m asl; leg. Chen, Hjalmarsson, Li, 9.viii.2013. BOLD Process ID SPHIM193-17, Field ID LZ05, Museum ID SMFTRI00018194.

Paratypes. 3 males, 1 female: Same data as holotype. Deposited in Senckenberg Research Institute, Frankfurt am Main, Germany (SMFTRI00017169, SMFTRI00017170, SMFTRI00017229) and Senckenberg Deutsches Entomologisches Institut, Müncheberg, Germany (SMFTRI00018193).

Additional material. 36 larvae: Same data as holotype. Deposited in Senckenberg Research Institute, Frankfurt am Main, Germany (Table S1).

Diagnosis. Males of the new species are most similar to those of *H. tibetana*, but (1) the dorsal margin of segment IX in lateral view is straight and evenly extending to the dorsomesal process (distally elevated with a distinct notch between segment IX and the dorsomesal process in *H. tibetana*); (2) the mesodorsal lobe of each superior appendage is sinuate and projecting dorsad (foliaceous, twisted, and projecting dorsocaudad in *H. tibetana*); (3) the proximal segment of each inferior appendage is longer than the superior appendages (about as long as the superior appendages in *H. tibetana*); (5) the distal segment of each inferior appendage has a distinct terminal indentation (with a shallow terminal indentation in *H. tibetana*); and (6) the dorsomesal process has strongly sclerotized and blunt tips without hooks (sclerotized tips with a small hook in *H. tibetana*). The female of the new species is most

similar to those of *H. maxima* and *H. tibetana* but (1) segment VIII is without lateral sutures (segment VIII has lateral sutures in *H. maxima*); (2) tergum IX is atrophied (tergum IX is present and triangular in *H. tibetana*); (3) the caudal margin of segment VIII in lateral view has an incision in the ventral portion (caudal margin of segment VIII in lateral view extends triangularly in *H. tibetana*).

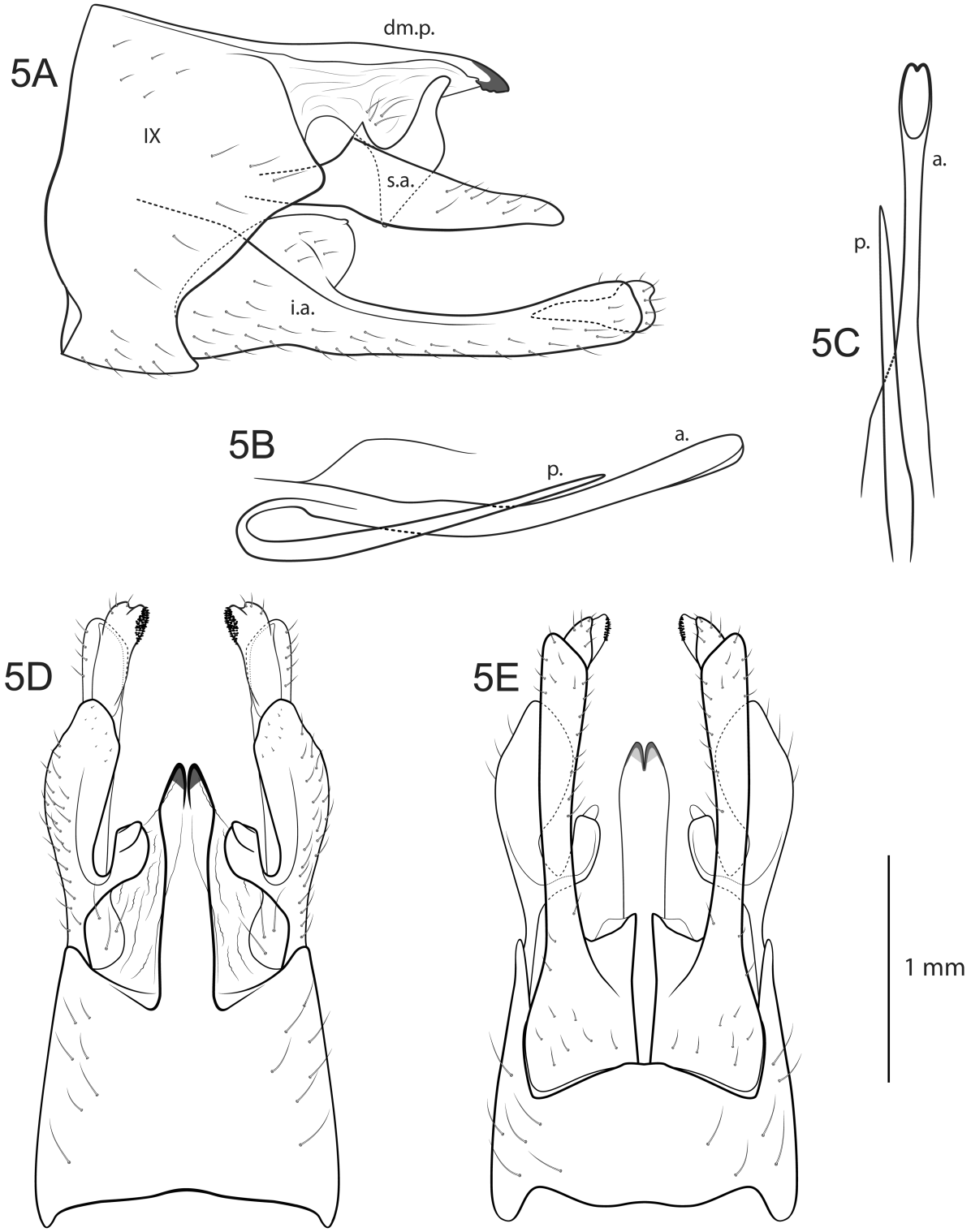

FIGURE 5. Male genitalia of *Himalopsyche velata* **sp. n.** 5A, left lateral; 5B, dorsal; 5C, ventral. Abbreviations: IX = abdominal segment IX; dm.p. = dorsomesal process; s.a. = superior appendages; i.a. = inferior appendages; a. = aedeagus; p. = paramere.

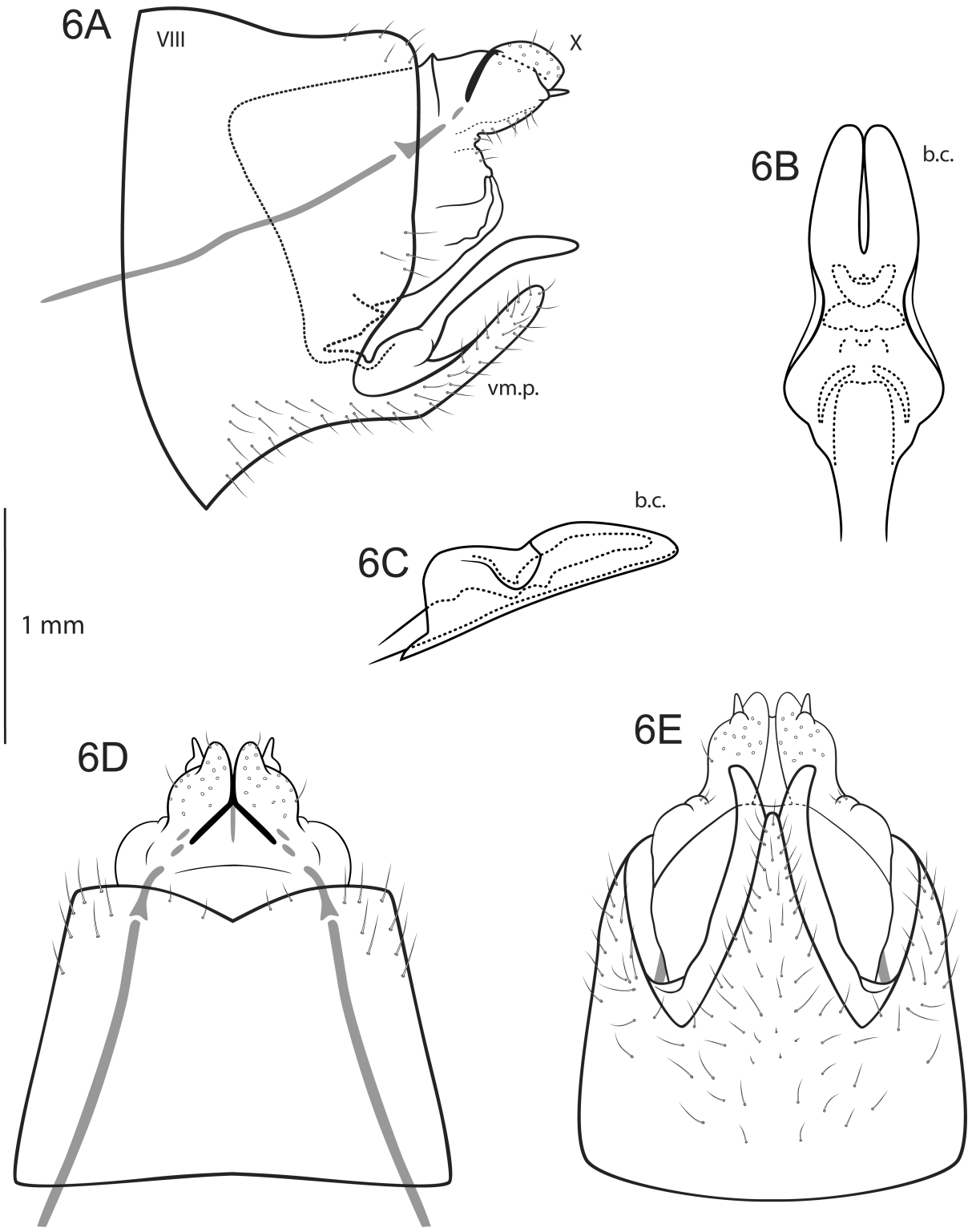

FIGURE 6. Female genitalia of *Himalopsyche velata* **sp. n.** 6A, left lateral; 6B, bursa copulatrix, dorsal; 6C, bursa copulatrix, left lateral; 6D, dorsal; 6E, ventral. Abbreviations: VIII = abdominal segment VIII; X = tergum X; b.c. = bursa copulatrix; vm.p. = ventromesal process of segment VIII.

Description. *Adults*. Habitus (in alcohol) light-brown; sternites beige, tergites brown; legs beige with dark stripes. Wings with light-brown pattern and dark setae on veins. Male maxillary palps each 5-segmented, spur formula 3-4-4. Length of each forewing in males 11–23 mm, in females 21–23 mm.

Male genitalia (Figure 5). Segment IX dorsally longer than ventrally and dorsomesally fused with tergum X, forming distinct dorsomesal process projecting caudad and with membranous region spanning between dorsomesal process and superior appendages (Figures 5A, 5D); segment IX in dorsal view anteriorly somewhat broader than caudally, anteriorly slightly concave, lateral margins straight, caudally concave (Figure 5D); in lateral view dorsal margin straight, upper caudal margin oblique and nearly straight with blunt dorsomesal apex and evenly rounded incision in ventral third (Figure 5A); in ventral view anteriorly slightly convex and sinuous with shallow incision mesally, caudally convex (Figure 5E). Dorsomesal process as long as tergum IX, in dorsal view slightly compressed at mid-length and widening distally to subrhombic apex, with pair of strongly sclerotized tips (Figure 5D); in lateral view with upper margin straight, slightly dilated in middle, and blunt tip projecting ventrocaudad (Figure 5A). Superior appendages each distinctly bilobed: Mesodorsal lobe projecting dorsad, in lateral view with caudal margin sinuate, its base longer than suddenly narrower terminal portion (Figure 5A), in dorsal view subrectangular with terminal portion projecting mesad and with clear incision between dorsomesal and lateral lobes (Figure 5D); lateral lobes longer than dorsomesal process but shorter than inferior appendages, subtriangular, projecting caudad, each with anterodorsal portion fused with membrane spanning from tergum X (Figure 5A), in dorsal view with lateral margins convex (Figure 5D). Inferior appendages each 2-segmented: Proximal segment bilobed, mesodorsal lobe in lateral view oval with minute dorsocaudal protuberance; lateroventral lobe digitiform and slightly dilating towards apex and with a distal segment attached mesodorsally; distal segment 1/4 as long as proximal segment and with bilobed tip, dorsal lobe of tip longer than ventral lobe and covered in fine dense thorns on dorsomesal face (Figures 5A, 5D, 5E). Aedeagus placed on left side of paramere, in lateral view digitiform, curving slightly dorsad, with long ventral opening at apex, connected with paramere in curve; in ventral view broad at base, tapering mesally and dilating towards tip, with opening long and with small incision at apex (Figure 5B, 5C). Paramere spiniform, thinner and shorter than aedeagus (Figure 5B, 5C).

Female genitalia (Figure 6). Segment VIII not divided into tergite and sternite, in dorsal view anteriorly broader than caudally, anterior margin slightly concave, lateral margins straight, oblique, caudal margin concave with mesal incision (Figure 6D); in lateral view higher anteriorly than caudally, dorsal margin slightly concave, dorsal portion of caudal margin straight, in the lower third incised and ventrally extending to a distinct digitiform ventromesal process covered with thick hairs projecting dorsocaudad and bearing a pair of finger-like ventromesal lobes covered in fine pubescent hairs, slightly bending and projecting caudad (Figure 6A); in ventral view anterior margin of segment VIII slightly convex, lateral margins straight and sweeping inward caudally, caudal margin with two distinct lateromesal incisions forming a triangular ventromesal process with two long and finger-like ventromesal lobes (Figure 6E). Tergum IX membranous and completely fused with tergum X. Tergum X membraneous with a dorsal fold and dorsal sclerites, dorsal lobes each bearing small cerci projecting caudad (Figures 6A, 6D, 6E). Apodemes jointed and connecting tergum X with segment VIII, extending anteriad (Figures 6A, 6D). Bursa copulatrix as pictured (Figures 6B, 6C).

Etymology. The word *velum* (sail) refers to the membraneous structure that is spanned, like a sail, between the dorsomesal process and the dorsomesal lobes of the superior appendages.

Distribution. Known from only the type locality (Figure 8A).

Discussion

The three newly described species are distinct in terms of both their morphology and genetic signal, and all occur in the Hengduan Mountains (Figure 8A). *Himalopsyche immodesta* and *H. velata* are both known from only the type locality. *Himalopsyche viteceki* is known from the type locality, as well as from Kachin Hills, Myanmar. *Himalopsyche velata* is morphologically most similar to *H. tibetana*, but judging from the phylogenetic tree generated by STACEY, it appears to be more closely related to *H. eos* and *H. auricularis* (Martynov 1914) and *H.* sp. 1196 (L) (Figure 1). *Himalopsyche viteceki* and *H. immodesta* were sister species in the phylogenetic analysis, and this sister pair formed a monophylum together with the *H. martynovi*-Complex and *H. epikur*.

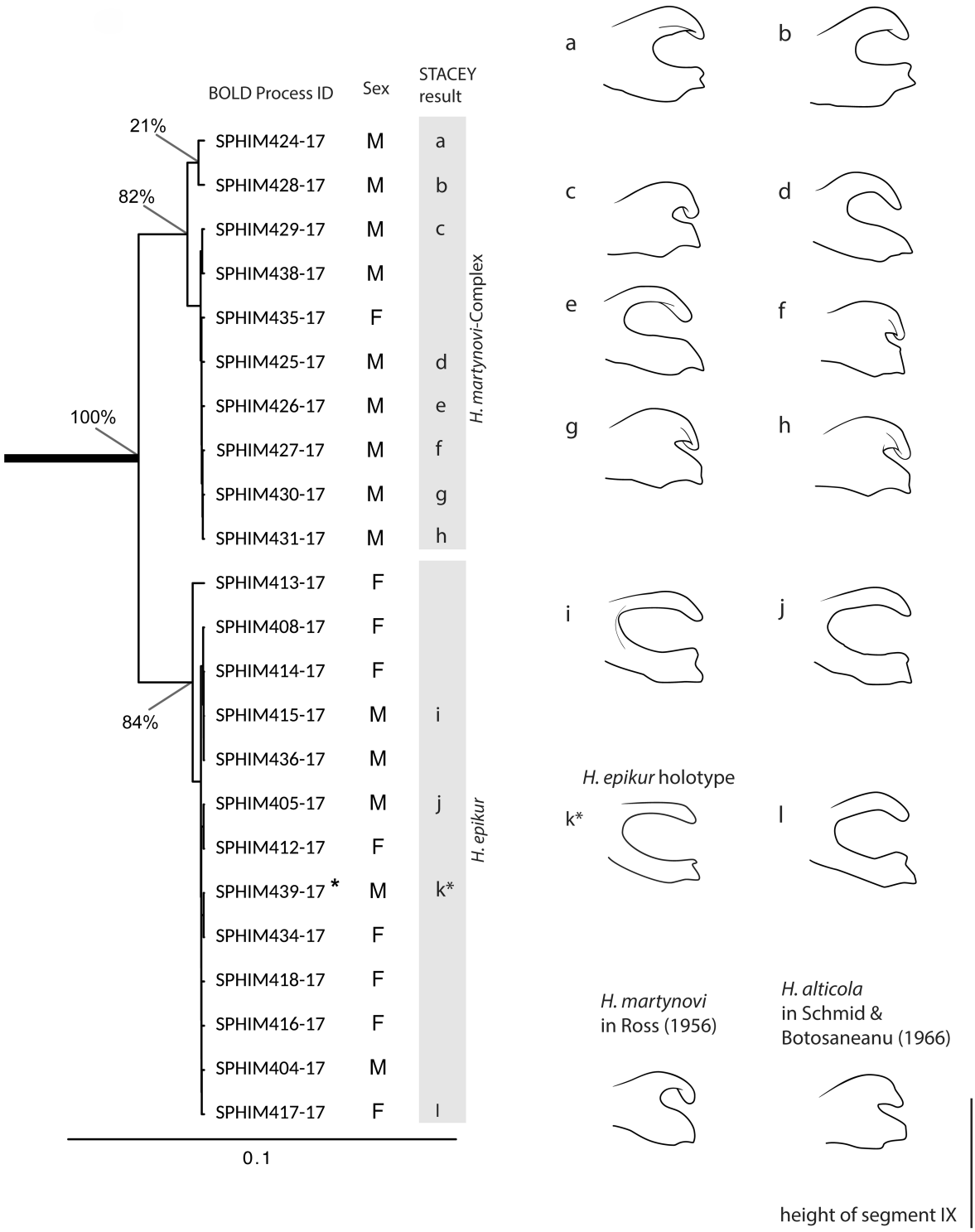

FIGURE 7. Morphological variation of the superior appendages of male genitals within the *H. martynovi*-Complex and *H. epikur*. Asterisk denotes the holotype of *H. epikur*. The topology is an excerpt from the tree generated with STACEY, which can be found in its completeness in Figure S1. Depictions of superior appendages are scaled to the height of abdominal segment IX. Scale bar indicates number of substitutions per unit branch length.

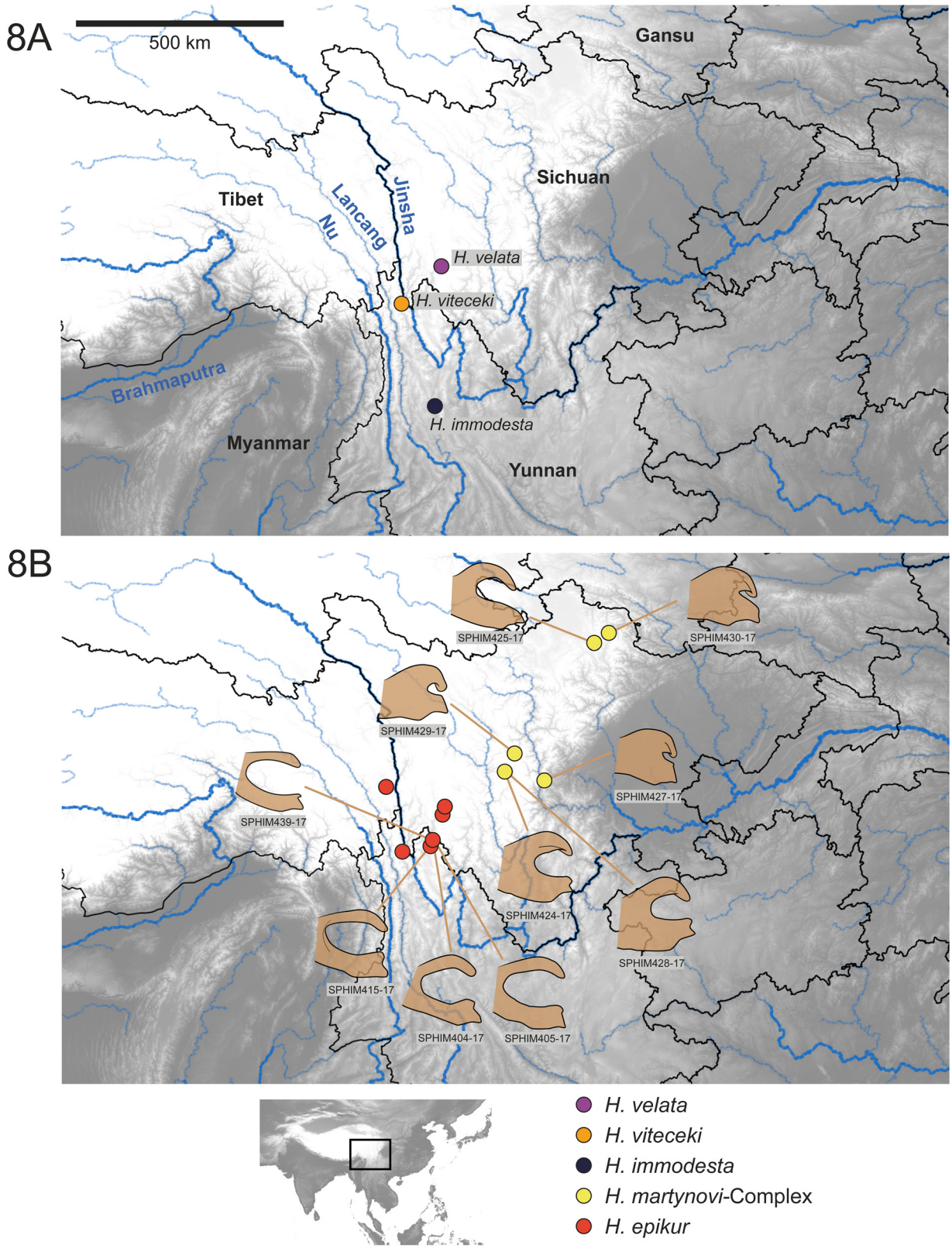

FIGURE 8. Maps of *Himalopsyche* spp. localities. 8A, type localities of *Himalopsyche viteceki* **sp. n.**, *H. immodesta* **sp. n.**, and *H. velata* sp.n.; 8B, sampling localities of specimens belonging to the *H. martynovi*-Complex and *H. epikur.*

Several species of *Himalopsyche* have a dorsomesal process extending from segment IX in the males (e.g., *H. triloba*, *H. lepcha*), and several species have a dorsomesal process of tergum X (e.g., *H. viteceki*), which can be more or less fused with segment IX (e.g., *H. martynovi*). The developmental origin of the dorsomesal process in *H. velata* is unknown and could be formed by segment IX, segment X, or both. I therefore refer to this structure as a dorsomesal process in order to avoid a terminology that suggests either developmental scenario for this structure, although my preferred hypothesis would be that the dorsomesal process in *H. velata* stems from tergum X, judging from the morphology of closely related species. The tips of this process are the anal sclerites according to Schmid and Botosanean (1966), however I refrain from defining them as such here since the origin of the dorsomesal process is unclear.

The species *H. alticola*, *H. martynovi*, and *H. epikur* were difficult to separate morphologically and genetically (Figure 7). There was one clade with specimens determined as *H. epikur* only, and for these specimens I consider the species determination to be reliable. For the specimens in the *H. martynovi*-Complex I consider the species determinations to be uncertain, but regard *H. martynovi* to be the most likely determination for all individuals of this clade (Table S1), thus there may not have been any true *H. alticola* present in the dataset. Figure 7 shows the morphological variation in the superior appendages in *H. epikur* and the *H. martynovi*-Complex, and these species appear to show morphological gradients. *Himalopsyche martynovi* and *H. alticola* were originally described in 1940 by Nathan Banks, but unfortunately the illustrations are not very detailed in the original descriptions; *H. martynovi* was later illustrated by Ross (1956), and *H. alticola* by Schmid & Botosaneanu (1966). *Himalopsyche martynovi* and *H. alticola* were described from Sichuan while *H. epikur* was described from Yunnan. When mapping the morphology of the superior appendages of the male genitalia, a geographic pattern is evident (Figure 8B). At this stage, it cannot be determined whether the three species represent a single evolving lineage with a geographic pattern or represent a case of ongoing speciation.

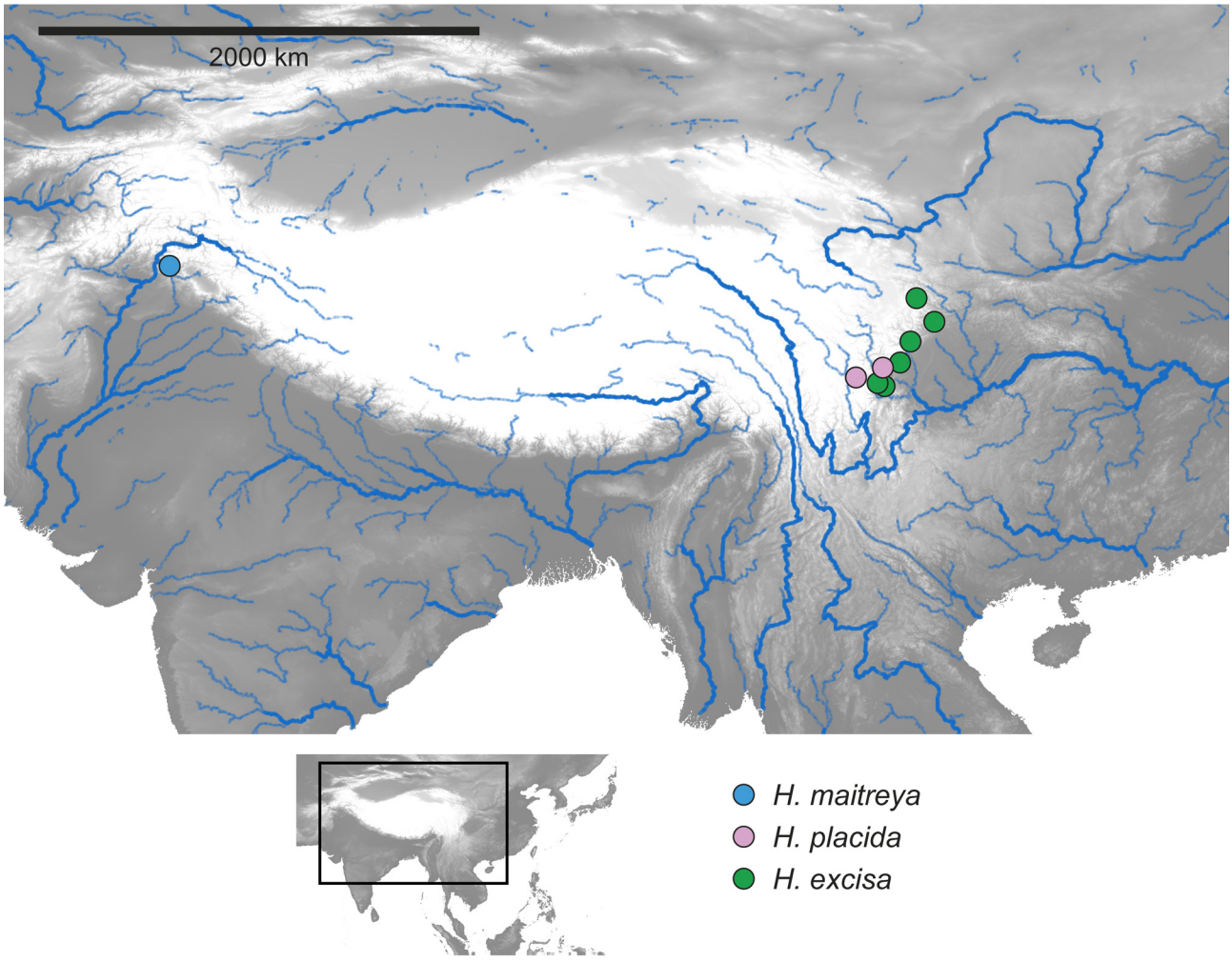

FIGURE 9. Map of sampling localities of *Himalopsyche* spp. belonging to the *H. excisa*-Complex.

Assuming that *H. epikur* and *H. martynovi* are separate species according to the species delimitation results, it appears that the sister species pairs *H. viteceki* and *H. immodesta*, and *H. epikur* and *H. martynovi*, have allopatric distributions (Figure 8B), and that sympatry occurs among non-sister species (e.g., *H. viteceki* and *H. epikur, and H. velata and H. epikur*). Although speculative at this stage, this pattern would fit into a model of allopatric speciation with secondary contact (Li *et al*. 2017).

STACEY analysis could not separate *H. excisa*, *H. maitreya*, and *H. placida* from one another and the morphological similarities among these species are striking. *Himalopsyche maitreya* is most distinct from the other two species, both geographically and morphologically. *Himalopsyche excisa* and *H. placida* occur in the Hengduan Mountains; *H. maitreya* is found in the Western Himalayas (Figure 9). A more-detailed study with additional material should clarify the status of the three nominal species.

Himalopsyche females display a large morphological variability among species, although taxonomy of females is less researched than that of the males. Within the *H. tibetana* Group (*sensu* Hjalmarsson *et al*. 2019), the following species have been described as females: *H. alticola* (detail), *H. anomala*, *H. digitata* Martynov 1935, *H. fasciolata* Kimmins 1952, *H. maitreya*, *H. maxima*, *H. tibetana*, and a specimen denoted "*H*. sp." by Schmid & Botosaneanu (Banks 1940; Forsslund 1935; Kimmins 1952; Lakhwinder & Saini 2015; Schmid & Botosaneanu 1966). The female of *H. anomala* Banks 1940 was described with a very simple illustration, and has, like its male counterpart, a very unique genital morphology. The females of *H. digitata*, *H. maitreya*, and *H*. sp. (*sensu* Schmid & Botosaneanu 1966) all share the common trait of a long ventromesal process extending from segment VIII. Females of *H. fasciolata*, *H. maxima*, *H. tibetana*, *H. velata*, and *H. viteceki* also have a ventromesal process, but it can be shorter and they also have a pair of ventromesal lobes attached to the ventromesal process.

In a life stage association analysis, Hjalmarsson *et al*. (2018) associated 33 larvae of *H. immodesta* and 36 larvae with *H. velata* based on two gene fragments. Larvae of *H. velata* were collected at type locality, where they occurred in abundance. Larvae of *H. immodesta* were collected at three localities in Yunnan. Hjalmarsson *et al*. (2018) could not identify larval traits that make determination of larvae to species level possible, but defined four larval types with a distinct morphology and corresponding to monophyletic groups (Hjalmarsson *et al.* 2019). In Supplementary Table S1, I list all the associated larvae of *H. immodesta* and *H. velata.*

The Hengduan Mountains are topographically and biologically very rich. Three majestic rivers (Nu, Lancang, and Jinsha) form massive gorges between glaciated mountains, creating steep gradients in the landscape. The region is quite young geologically (around 8 million years old) and recent uplift may have promoted speciation in this area (Favre *et al* 2015; Hoorn *et al*. 2013; Xing & Ree 2017). We know very little about the distribution and ecology of the newly described species, and more intense faunistic work in the area is desirable. This study illustrates the significance of the Hengduan Mountains as a potential source of yet-undiscovered biodiversity.

Acknowledgements

I thank Hans Malicky (Lunz am See, Austria) and Wolfram Mey (Berlin, Germany) for providing valuable specimens. Field work and molecular work were funded by DFG Grant PA1617/2-1. I thank Ram Devi Tachamo Shah, Deep Narayan Shah, Fengqing Li, Subdoh Sharma, Qinghua Cai, Xiaoli Tong, Felicitas Hoppeler, Steffen Pauls, and Sonja Jähnig for their contributions in the field, and Jürgen Otte for his assistance with DNA extractions. I thank Simon Vitecek for his consultancy and feedback with species descriptions and illustrations, Steffen Pauls for comments on the manuscript, and one anonymous reviewer as well as John Morse for invaluable feedback on the manuscript.

References

Banks, N. (1940) Report on certain groups of neuropteroid insects from Szechwan, China. *Proceedings of the United Stated National Museum*, 88, 173–220.
https://doi.org/10.5479/si.00963801.88-3079.173

Banks, N. (1947) Some neuropterous insects from Szechwan, China. *Fieldiana-Zoology*, *Chicago Natural History Museum*, 31, 97–107.
https://doi.org/10.5962/bhl.title.2821

Blahnik, R.J., Holzenthal, R.W. & Prather, A. (2007) The lactic acid method for clearing Trichoptera genitalia. *In*: Bueno-Soria, J., Barba-Álvarez, R. & Armitage, B. (Eds.), *Proceedings of the XIIth International Symposium on Trichoptera*, *18–22 June*, *2006*. The Caddis Press, Columbus, Ohio, pp. 9–14.

Bouckaert, R. & Drummond, A. (2017) bModelTest: Bayesian phylogenetic site model averaging and model comparison. *BMC Evolutionary Biology*, 17, 42.
https://doi.org/10.1186/s12862-017-0890-6

Bouckaert, R., Heled, J., Kühnert, D., Vaughan, T., Wu, C.-H., Xie, D., Suchard, M.A., Rambaut, A. & Drummond, A.J. (2014) BEAST 2: A Software Platform for Bayesian Evolutionary Analysis. *PLoS Computational Biology*, 10 (4), e1003537.
https://doi.org/10.1371/journal.pcbi.1003537

Favre, A., Päckert, M., Pauls, S.U., Jähnig, S.C., Uhl, D., Michalak, I. & Muellner-Riehl, A.N. (2015) The role of the uplift of the Qinghai-Tibetan Plateau for the evolution of Tibetan biotas. *Biological Reviews*, 90, 236–253.
https://doi.org/10.1111/brv.12107

Flint, O.S. (1961) The presumed larva of *Himalopsyche phryganea* (Ross) (Trichoptera: Rhyacophilidae). *The Pan-Pacific Entomologist*, 37, 199–202.

Forsslund, H.K. (1935) Schwedisch-chinesische wissenschaftliche Expedition nach den nordwestlichen Provinzen Chinas. *Arkiv för Zoologi*, 1 (31), 1–21.

Fujisawa, T. & Barraclough, T.G. (2013) Delimiting species using single-locus data and the generalized mixed yule coalescent approach: A revised method and evaluation on simulated data sets. *Systematic Biology*, 62, 707–724.
https://doi.org/10.1093/sysbio/syt033

Graf, W. & Sharma, S. (1998) The larva of *Himalopsyche tibetana* (Insecta: Trichoptera, Rhyacophilidae) with some ecological notes on the genus *Himalopsyche* Banks, 1940 from Nepal. *In*: Chalise, S.R. & Khanal, N.R. (Eds.), *International Conference on Ecohydrology of High Mountain Areas.* International Centre for Integrated Mountain Development, Kathmandu, pp. 561–571.

Hjalmarsson, A.E., Graf, W., Jähnig, S., Cai, Q., Tong, X., Li, F., Tachamo Shah, R.D., Narayan Shah, D., Sharma, S. & Pauls, S.U. (2018) Life stage association and morphological characterization of larval types of *Himalopsyche* (Trichoptera: Rhyacophilidae). *ZooKeys*, 773, 79–108.
https://doi.org/10.3897/zookeys.773.24319

Hjalmarsson, A.E., Graf, W., Vitecek, S., Jähnig, S.C., Cai, Q., Sharma, S., Tong, X., Li, F., Narayan Shah, D., Tachamo Shah, R.D. & Pauls, S.U. (2019) Molecular phylogeny of *Himalopsyche* (Trichoptera, Rhyacophilidae). *Systematic Entomology* (early view).
https://doi.org/10.1111/syen.12367

Hoorn, C., Mosbrugger, V., Mulch, A. & Antonelli, A. (2013) Biodiversity from mountain building. *Nature Geoscience*, 6, 154–154.
https://doi.org/10.1038/ngeo1742

Hsu, L.P. (1997) *A taxonomic study of Trichoptera from Taiwan (Insecta)*. Ph.D. Dissertation, Tokai University, Taipei 370 pp. [in Chinese with English abstract]

Jokusch, E.L., Martínez-Solano, I. & Timpe, E.K. (2014) The effects of inference method, population sampling, and gene sampling on species tree inferences: An empirical study in slender salamanders (Plethodontidae: *Batrachoseps*). *Systematic Biology*, 64, 66–83.
https://doi.org/10.1093/sysbio/syu078

Jones, G. (2017) Algorithmic improvements to species delimitation and phylogeny estimation under the multispecies coalescent. *Journal of Mathematical Biology*, 74, 447–467.
https://doi.org/10.1007/s00285-016-1034-0

Jones, G., Aydin, Z. & Oxelman, B. (2015) DISSECT: An assignment-free Bayesian discovery method for species delimitation under the multispecies coalescent. *Bioinformatics*, 31, 991–998.
https://doi.org/10.1093/bioinformatics/btu770

Katoh, K., Misawa, K., Kuma, K. & Miyata, T. (2002) MAFFT: A novel method for rapid multiple sequence alignment based on fast Fourier transform. *Nucleic Acids Research*, 30 (14), 3059–3066.
https://doi.org/10.1093/nar/gkf436

Kawai T. & Tanida, K. (2005) *Aquatic Insects of Japan*: *Manual with Keys and Illustrations*. Tokai University Press, Kanagawa, 1342 pp. [in Japanese]

Kimmins, D.E. (1952) XL.—Indian caddis flies.—VI. New species and a new genus of the subfamily Rhyacophilinae. *Annals and Magazine of Natural History*, Series 12, 5 (52), 347–361.
https://doi.org/10.1080/00222935208654302

Lakhwinder, K. & Saini, M.S. (2015) A new species of the genus Himalopsyche (Trichoptera, Rhyacophilidae), with key to and catalogue of Indian species. *Vestnik zoologii*, 49, 3–12.

Larsson, A. (2014) AliView: A fast and lightweight alignment viewer and editor for large data sets. *Bioinformatics*, 30 (22), 3276–3278.
https://doi.org/10.1093/bioinformatics/btu531

Lepneva, S.G. (1970) *Fauna of the U.S.S.R., Trichoptera, Volume II No. 1, Larvae and Pupae of Annulipalpia*. Smithsonian Institution and the National Science Foundation, Washington, D.C., 656 pp.

Li, X., Jiang, N., Cheng, R., Xue, D., Qu, Y. & Han, H. (2017) Allopatric divergence and secondary contact without genetic admixture for *Arichanna perimelaina* (Lepidoptera: Geometridae), an alpine moth endemic to the Hengduan Mountains.

Systematic Entomology, 42, 703–713.
https://doi.org/10.1111/syen.12234
Malicky, H. (1978) Beiträge zur Kenntnis der Insektenfauna Sumatras. Teil 7: Köcherfliegen (Trichoptera) aus Sumatra und West-Neuguinea I. Rhyacophilidae, Glossosomatidae, Stenopsychidae, Goeridae. *Beiträge zur naturkundlichen Forschung in Südwestdeutschland*, 37, 159–173.
Malicky, H. (2000) Einige neue Köcherfliegen aus Sabah, Nepal, Indien und China (Trichoptera: Rhyacophilidae, Hydrobiosidae, Philopotamidae, Polycentropodidae, Ecnomidae, Psychomyiidae, Hydropsychidae, Brachycentridae, Odontoceridae, Molannidae). *Braueria*, 27, 32–39.
Malicky, H. (2011) Neue Trichopteren aus Europa und Asien. *Braueria*, 38, 23–43.
Martynov, A.V. (1914) Contributions a la faune des Trichoptères de la Chine. *Annuaire du Musée Zoologique de l'Académie Impériale des Sciences de Saint Pétersbourg*, 19, 323–339.
Martynov, A.V. (1930) On the trichopterous fauna of China and Eastern Tibet. *Proceedings of the Zoological Society of London*, 5, 65–112.
https://doi.org/10.1111/j.1096-3642.1930.tb00967.x
Martynov, A.B. (1935) On a collection of Trichoptera from the Indian Museum. Part I.—Annulipalpia. *Records of the Indian Museum*, 37, 93–306.
Rannala, B. (2005) The art and science of species delimitation *Current Zoology*, 61, 846–853.
https://doi.org/10.1093/czoolo/61.5.846
Ross, H.H. (1956) *Evolution and Classification of the Mountain Caddisflies*. University of Illinois Press, Urbana, pp.
Saini, M.S. & Kaur, L. (2011) Revised phylogenetic analysis of Indian species of genus *Himalopsyche* Banks (Trichoptera: Spicipalpia: Rhyacophilidae). *Halteres*, 3, 26–29.
Saito, T. 1965. Larvae of two fresh water insects, *Himalopsyche japonica* and *Neohapalothrix kanii*. *Report of the Japanese Society of Systematic Zoology*, 1, 14–16.
Schlick-Steiner, B.C., Steiner, F.M., Seifert, B., Stauffer, C., Christian, E. & Crozier, R.H. (2010) Integrative taxonomy: A multisource approach to exploring biodiversity. *Annual Review of Entomology*, 55 (1), 421–438.
https://doi.org/10.1146/annurev-ento-112408-085432
Schmid, F. (1963) Quelques *Himalopsyche* indiènnes (Trichoptères, Rhyacophilidae). *Bonner Zoologische Beiträge*, 14, 206–223.
Schmid, F. (1969) *Sur trois Himalopsyche d'URSS* (Trichoptères, Rhyacophilides). *Le Naturaliste Canadien*, 96, 243–346.
Schmid, F. (1970) Le genre Rhyacophila et la famille des Rhyacophilidae (Trichotera). *Mémoires de la Société Entomologique du Canada*, 66, 1–230.
https://doi.org/10.4039/entm10266fv
Schmid, F. & Botosaneanu, L. (1966) Le genre *Himalopsyche* Banks (Trichoptera, Rhyacophilidae). *Annales de la Société entomologique du Québec*, 11, 123–176.
Tanida, K. (1985) Trichoptera. *In*: Kawai, T. (Ed.), *An Illustrated Book of Aquatic Insects of Japan*. Tokai University Press, Tokyo, pp. 167–215.
Thamsenanupap P., Chantaramongkol, P. & Malicky, H. (2005) Description of caddis larvae (Trichoptera) from northern Thailand of the genera *Himalopsyche* (Rhyacophilidae), *Arctopsyche* (Arctopsychidae), cf. *Eoneureclipsis* (Psychomyiidae) and *Inthanopsyche* (Odontoceridae). *Braueria*, 32, 7–11.
Ulmer, G. (1905) Neue und wenig bekannte Trichopteren der Museen zu Brussel und Paris. *Annales de la Société Entomologique de Belgique*, 49, 17–42.
Vitecek, S., Kučinić, M., Previšić, A., Živić, I., Stojanović, K., Keresztes, L., Bálint, M., Hoppeler, F., Waringer, J., Graf, W. & Pauls, S.U. (2017) Integrative taxonomy by molecular species delimitation: Multi-locus data corroborate a new species of Balkan Drusinae micro-endemics. *BMC Evolutionary Biology*, 17, 129.
https://doi.org/10.1186/s12862-017-0972-5
Xing, Y. & Ree, R.H. (2017) Uplift-driven diversification in the Hengduan Mountains, a temperate biodiversity hotspot. *Proceedings of the National Academy of Sciences*, 114 (17), E3444–E3451.
https://doi.org/10.1073/pnas.1616063114
Yang, Z. & Rannala, B.H. (2010) Bayesian species delimitation using multilocus sequence data. *Proceedings of the National Academy of Sciences*, 107, 9264–9269.
https://doi.org/10.1073/pnas.0913022107
Zhang, J., Kapli, P., Pavlidis, P. & Stamatakis, A. (2013) A general species delimitation method with applications to phylogenetic placements. *Bioinformatics*, 29 (12), 2869–2876.
https://doi.org/10.1093/bioinformatics/btt499

Figure S1

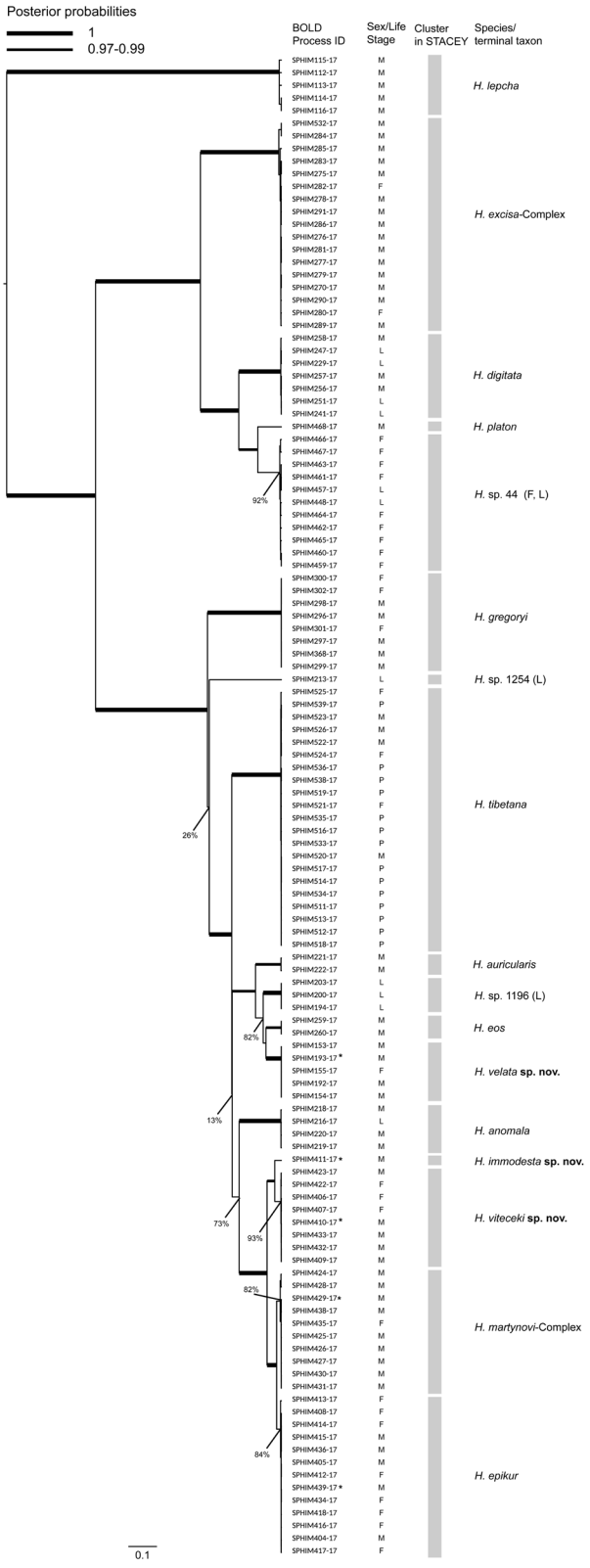

FIGURE S1. Detailed species tree showing the complete topology with the BOLD Process IDs and sex/life stages of each sample. Branch thicknesses indicate posterior probabilities of clades, for those with a posterior probability value of at least 97%; nodes with lower posterior probabilities are annotated. Posterior probabilities for nodes within STACEY clusters are not shown. Sexes/life stages are denoted as follows. F = female; L = larva; M = male; P = pupa. Scale bar indicates number of substitutions per unit branch length. Asterisks denote holotypes.

Supplementary material for online publication only

TABLE S1 List of all samples, their catalogue numbers, species identities, locality information, and sequence lengths. The following abbreviations are used. Life Stage: F = female; L = larva; M = male; P = pupa. Institution Storing: HM = Research collection of Hans Malicky, Lunz am See, Austria; MFN = Museum für Naturkunde, Berlin, Germany; SGN Frankfurt a. M. = Senckengberg Research Institute, Frankfurt am Main, Germany, SGN Müncheberg = Senckenberg Research Institute and Natural History Museum, Müncheberg, Germany. (Please see the publication page for Table S1).